MULTI-BEAM LASER HEATING OF STEEL: TEMPERATURE AND THERMAL STRESS ANALYSIS

Shahzada Zaman Shuja, Bekir Sami Yilbas
Mechanical Engineering Department, King Fahd University of Petroleum and Minerals, Dhahran, Saudi Arabia
E-mail: shuja@kfupm.edu.sa; bsyilbas@kfupm.edu.sa

Received April 2012, Accepted January 2013
No. 12-CSME-46, E.I.C. Accession 3366

ABSTRACT

Laser multi-beam heating of steel sheet surface is considered. The irradiated laser spots are located along an arc to increase heated surface area during laser scanning at a constant speed. Temperature and stress fields are predicted for various number of spots along the arc. It is found that temperature and stress fields in the irradiated substrate can be controlled through proper selection of the number of irradiated spots along the arc. Increasing number of irradiated spots results in development of almost uniform high temperature and high stress fields around the arc; however, local heating and discontinuous stress field giving rise to large differences in von Mises stress occurring for reduced number of spots in the arc.

Keywords: laser; heating; multi-beam; thermal stress.

CHAUFFAGE PAR LASER MULTI-FAISCEAU D'UNE PIÈCE EN ACIER : ANALYSE DE LA TEMPÉRATURE ET DU STRESS THERMIQUE

RÉSUMÉ

Le chauffage par laser multi-faisceau d'une pièce en acier est l'objet de l'étude. Les taches laser irradiées sont situées le long d'un arc pour augmenter l'aire de la surface chauffée durant le balayage laser à une vitesse constante. La température et les champs de stress sont estimés sur diverses taches le long de l'arc. On a constaté que la température et les champs de stress dans le substrat irradié peuvent être contrôlés par une sélection adéquate du nombre de taches irradiées le long de l'arc. L'augmentation du nombre de taches irradiées entraîne un développement presque uniforme de température élevée et de stress le long de l'arc. Cependant, le chauffage localisé et le stress discontinu du champ génèrent de grandes différences des contraintes von Mises produites par un nombre réduit de taches le long de l'arc.

Mots-clés : laser ; chauffage ; multi-faisceau ; stress thermique.

1. INTRODUCTION

Lasers can be used as effective tool to heat metal surfaces. Laser heating has several advantages over conventional heating methods including plasma arc and Oxy-fuel heating. Some of these advantages include precise operation, local treatment, fast processing, and low cost. Laser processing can be categorized mainly into two groups, which include conduction limited and non-conduction limited processing. In conduction limited processing material is heated below the melting temperature and high cooling rates result in quenching effect generating high thermal stress in the heated region. Non-conduction limited processing involves change process to make the workpiece easier to machine, weld, clad, etc. Because laser heating is applied during a short time period to limited surface regions determining stress fields experimentally would be difficult and expensive if not practical. Numerical simulation of the heating to map stress as well as temperature distribution provides physical insight into the thermal process that takes place during the heating cycle. In addition, thermal stress field can be controlled through multi multi-beam laser scanning of the workpiece; in which case, the orientation of multi-beams at the surface determines the minimum stress intensity in the heated region. Consequently, investigation into laser multi-beam heating of the metallic surfaces becomes essential to minimize thermal stresses.

Considerable research has been carried out to study the laser heating process. Laser heating and forming of light weight structures were studied by Araghi et al. [1]. They introduced liquid sheet forming process incorporating laser processing, which enabled to form individual parts those used in the particular aerospace industry. Influence of laser scanning lines on stress levels in a treated sheet metal was investigated by Dean and Zhang [2]. They showed that influence of scanning lines on stress levels was notably high, which was associated with microstructural changes in the heated region. Laser heating of metallic sheets was examined by Boley et al. [3] They indicated that as laser softens the metallic sheet during the heating period and pressure difference between the front and back surface of the workpiece due to high pressure air blow caused the workpiece to bulge into the shape desired. A model study for laser bending of pre-loaded sheet metals was carried out by Guon et al. [4]. Their findings revealed that forming performance could be improved significantly under pre-stress conditions, and the deformation direction could also be controlled easily by changing the direction and the value of the pre-loading. Laser produced overlapped scan tracks to increase strength and rigidity of sheet metals were studied by Schimek et al. [5]. They showed that fatigue strength of the treated workpiece depended on geometric orientations of scan tracks at the surface. Laser induced sheet metal forming was investigated by Ueda et al. [6]. They indicated that preformed residual stresses at the sheet metal surface changed from a large compressive stress to a small tensile stress after laser treatment process. Laser annealing of metallic films was examined by Chen et al. [7]. Their findings showed that laser beam profile greatly affected the surface roughness of laser treated film. Nd:YAG laser cladding of metallic surfaces was studied by Kim et al. [8]. They indicated that a desired shape of surface profile could be achieved through proper selection of cladding parameters.

In the present study, laser multi-beam heating of thin steel sheet is considered. Temperature and stress fields are simulated numerically in the heated region. The influence of number of laser spots on thermal stress field is evaluated.

2. MATHEMATICAL ANALYSIS

Figure 1 shows laser heating situation and the coordinate system used in simulations.

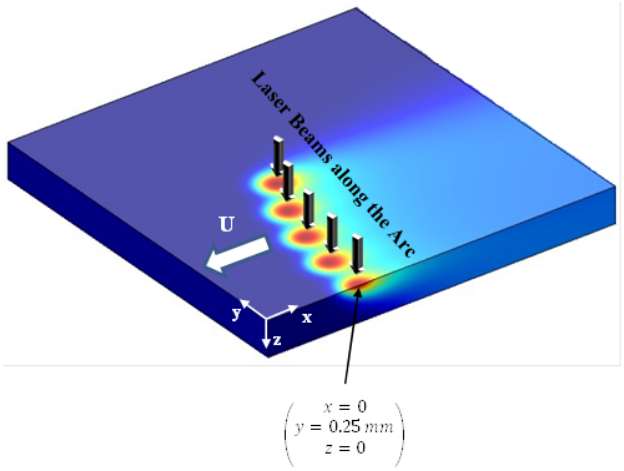

(a)

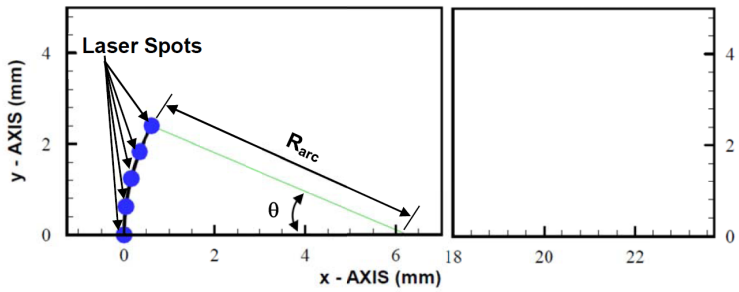

(b)

Fig. 1. A schematic view of laser spots along the arc: (a) the coordinate system, (b) top view of the workpiece and its size along with the laser spots.

2.1. Laser Heating

Laser heating of a steel sheet is considered such that laser scans the surface at a constant speed (U) along the x-axis (Fig. 1). The enthalpy equation governing laser heating process can be written as:

$$\rho\frac{\partial H}{\partial T} + \nabla\cdot(\rho U H) = \nabla\cdot(k\nabla T) + S_0\,, \tag{1}$$

where H is the enthalpy, ρ is the density, U is the laser beam scanning velocity, k is the thermal conductivity, and S_o is the volumetric source term, resembling the absorption of the laser beam, due to the laser spots located around the arc. The moving source consideration allows reducing the transient heating to a quasi-steady or a steady heating situation; in which case, the temporal term in Eq. (1) vanishes. The laser beam axis is the z-axis (Fig. 1a) and the laser beam scans at the surface along the x- axis. The volumetric source resembling the absorption of the incident beam is:

$$S_0 = \sum_{n=0}^{n=nss} I_0\delta\left(1-r_f\right)\exp\left(-\delta z\right)\exp\left(-\left(\frac{\sqrt{(x-x_n)^2+(y-y_n)^2}}{a}\right)^2\right)\,, \tag{2}$$

where I_o is laser peak intensity, δ is the absorption coefficient, a is the Gaussian parameter ($a = 0.0002$ m), r_f is the surface reflectivity, x and y are the axes (Fig. 1a), $nss = \frac{ns-1}{2}$ (ns is total number of laser spots, $ns = 7, 9, 11, 13, 25$), n is the laser spot number, x_n and y_n are defined as: $x_n = R_{arc}(1 - \cos(\frac{n\theta}{nss}))$ and $y_n = R_{arc}(1 - \sin(\frac{n\theta}{nss}))$. Here, R_{arc} is the arc radius (Fig. 1b, $\theta = \frac{s}{R_{arc}}$ and $s = \frac{R_{arc}}{2}$). Laser intensity is kept the same at the first and at the second spots in the simulations.

In order to solve Eq. 1, two boundary conditions for each principal axis should be specified. Convection heat loss is the same as the conduction flux at the surface, i.e:

The convection heat flux across the irradiated surface is:

$$k\frac{\partial T(x, y, 0, t)}{\partial z} = h_t\,(T_s - T_\infty)\ , \tag{3}$$

where h_t is the heat transfer coefficient at the free surface. The heat transfer coefficient predicted earlier [9] is used in the present simulations across the heated spots ($h_t = 3 \times 10^3$ W/m^{2}K) due to the jet impingement and the other regions at the surface, the natural convection is considered ($h_t = 10$ W/m^{2}K) to account for the cooling. It should be noted that high value of heat transfer coefficient at the free surface of the workpiece resembles the convection effect of assisting gas jet that impinges onto the surface.

The other boundary conditions, therefore, are:

$$z \text{ at bottom surface:} \quad z = z_{th}\text{:} \quad -\frac{\partial T\,(x, y, z_{th}, t)}{\partial z} = \frac{h_t}{k}\left(T_{s,b} - T_\infty\right)\ , \tag{4}$$

where z_{th} is the workpiece thickness, h_t is the heat transfer coefficient due to natural convection ($h_t = 10$ W/m^{2}K) and $T_{s,b}$ is the surface temperature at the workpiece bottom surface.

$$x \text{ at infinity:} \quad x = \pm\infty\text{:} \quad T(\pm\infty, y, z, t) = T_o \text{ (specified)}\,, \tag{5}$$

$$y \text{ at outer edge:} \quad y = y_{width}\text{:} \quad \frac{\partial T(x, y_{width}, z, t)}{\partial y} = \frac{h}{k}\left(T_{s,w} - T_\infty\right)\ , \tag{6}$$

where y_{width} is the half width of the workpiece and $T_{s,w}$ is temperature at the outer edge of the workpiece.

$$y \text{ at the symmetry plane:} \quad y = 0\text{:} \quad \frac{\partial T(x, 0, z, t)}{\partial y} = 0\,. \tag{7}$$

2.2. Thermal Stress

For structural response, finite element formulation is incorporated, which is based on the principle of virtual work. From the principle of virtual work (PVW), a virtual (very small) change of the internal strain energy (δU) must be offset by an identical change in external work due to the applied loads (δV). Considering the strain energy due to thermal stresses resulting from the constrained motion of a body during a temperature change, PVW yields:

$$\{\delta\mathbf{u}\}^T \int\limits_{vol} [B]^T\,[D]\,[B]\,dv\,\{\mathbf{u}\} = \{\delta\mathbf{u}\}^T \int\limits_{vol} [B]^T\,[D]\left\{\boldsymbol{\varepsilon}^{th}\right\} dv\,. \tag{8}$$

Noting that the $\{\delta\mathbf{u}\}^T$ vector is a set of arbitrary virtual displacements common in all of the above terms, the condition required to satisfy above equation reduces to:

$$[K]\,\{\mathbf{u}\} = \left\{\mathbf{F}^{th}\right\}\ , \tag{9}$$

where

$[K] = \int_{vol} [B]^T [D][B] dv$ =Element stiffness matrix,

$\left\{\mathbf{F}^{th}\right\} = \int_{vol} [B]^T [D] \left\{\boldsymbol{\varepsilon}^{th}\right\} dv$ =Element thermal load vector,

$\left\{\boldsymbol{\varepsilon}^{th}\right\} = \{\boldsymbol{\alpha}\} \Delta T$ =Thermal strain vector,

$\{\boldsymbol{\alpha}\}$ =Vector of coefficients of thermal expansion.

In the present study, effect of mechanical deformation on heat flow has been ignored and the thermo-mechanical phenomenon of heating is idealized as a sequentially-coupled unidirectional problem. Conducting solid element is used in the thermal analysis. Conducting solid element is also analyzed structurally; therefore, the element is replaced by an equivalent structural element for the structural analysis. The element has plasticity, creep, swelling, stress stiffening, large deflection, and large strain capabilities.

2.3. Numerical Solution

Finite element model is used to solve Eqs. (1) and (8). COMSOL Finite Element Code is used in the simulations. A non-uniform rectangular grid is used with 100×150 cells. The grids are dense near the heat sources in order to accurately resolve for temperature and stress distributions. The solver was run until the converged results were obtained. In this case, the residual error for the energy equation was less than the limit set in the simulations, which is 10^{-8}. It should be noted that the error related to the predictions is minimized through setting the residual error in the energy equation in COMSOL.

Laser spots along the arc are considered to examine the influence of the laser spots on temperature field at the workpiece surface. In this case, number of spots 7, 9, 11, 13 and 15 are equally spaced around the arc (Fig. 1b), which moves at a constant scanning speed of 0.1 m/s. Laser parameters used in the simulations are given in Table 1 while Table 2 gives the thermal properties of steel used in the simulations.

Intensity (W/m^2)	Scanning speed (m/s)	Gaussian parameter "a" (m)	Number of laser spots
2×10^8	0.1	0.0002	7, 9, 11, 13, 15

Table 1. Laser parameters used in the simulations.

3. RESULTS AND DISCUSSION

Laser multi-beam heating of steel sheet is carried out. Temperature and stress fields are evaluated in the irradiated region for various spot sizes.

Figure 2 shows contour plots of temperature and stress fields in steel sheet when laser beam scans the surface at a constant speed. Since conduction limited heating is considered, laser power intensities at the irradiated spot center are fixed to generate surface temperature below the melting temperature of the substrate material. Equally spaced spots are located in the arch and they move along the x-axis with a constant speed. Influence of number of laser spots on temperature field becomes less significant as the number of spots along the arc reduces. In the case of seven spots in the arc, temperature contours due to each beam does not

Specific heat capacity (J/kgK)	$109.2 + 2.57*T - 0.00653*T^2$
Thermal conductivity (W/mK)	$6.742 + 0.0286*T$
Density (kg/m^3)	$7945.3 - 0.2*T$
Absorption coefficient (l/m)$\times 10^7$	6.17
Thermal expansion coefficient (l/K)	$1.356 \times 10^{-5} + 6.95 \times 10^{-9}*T$
Elastic modulus (Pa)	$2.24 \times 10^{11} - 8.93 \times 10^7*T$
Poisson's ratio	$0.265 + 8.22 \times 10^5*T$

Table 2. Thermal properties of the workpiece used in the simulations [9].

overlap in the high temperature region at the surface. In this case, each laser spot acts like individual heat source causing local heated region at the surface. As the number of laser spots increases, high temperature contours overlaps at the surface resulting in almost continuous temperature contours along the arc as if the heating is carried out by a single arch shaped laser beam profile. Moreover, this also provides wide coverage of heating area at the surface rather than using an equivalent single laser beam of one spot. However, single beam of one spot having a total power intensity of the multi-beams could not result high temperature region covering a large area, it rather causes a phase at the surface modifying the conduction limited laser treatment at the surface. In the case of thermal stress field, seven spots around arc results in stress centers in the area of each irradiated spot. This is because of the high temperature gradients formed across each spot, since temperature field is not continuous along the arc.

Increasing number of spots results in continuity of high temperature region along the arc. This is related to development of relatively lower temperature gradient along the arc as compared to that corresponding to few irradiated spots. Consequently, high stress field becomes almost continuous along the arc with increasing number of spots. Stress level becomes lower along the arc for large number of spots than that corresponding to few spots at the surface. However, the high temperature gradient formed in the neighborhood of the irradiated spots gives rise to attainment of high stress levels in these regions despite the presence of low stress levels along the arc.

Figure 3 shows temperature distribution along the arc for different number of laser irradiated spots. The difference in the maximum and the minimum temperature is considerably high for 7 irradiated spots at the surface. Large difference indicates that overlapping of heated regions between the irradiated spots is small. Therefore, temperature uniformity along the arc, where the irradiated spots are situated, becomes less likely. Consequently, the temperature gradients in the edges of the irradiated spots become high. As the number of laser spots along the arc increases, temperature difference between the maximum and the minimum temperatures becomes small. This is more pronounced for 15 laser spots at the surface. Although complete overlapping of temperature field is not evident, temperature difference along the arc is small, which can be considered as homogeneous temperature distribution along the arc. Therefore, the temperature gradient is expected to be rather smaller at the edges of the irradiated spot along the arc. Figure 4 shows von Mises stress variation along the arc for various numbers of irradiated spots. von Mises stress attains high values in the region of the large temperature gradients. The difference between the maximum and the minimum von Mises stress is large for 7 irradiated spots at the surface. This difference is on the order of 400 MPa which is considered to be high across the small distances along the arc. The difference in von Mises stress increases slightly towards the end of the arc. This is associated with high rate of heat conduction towards this region while resulting in high temperature gradients in the arc end region. von Mises stress increases

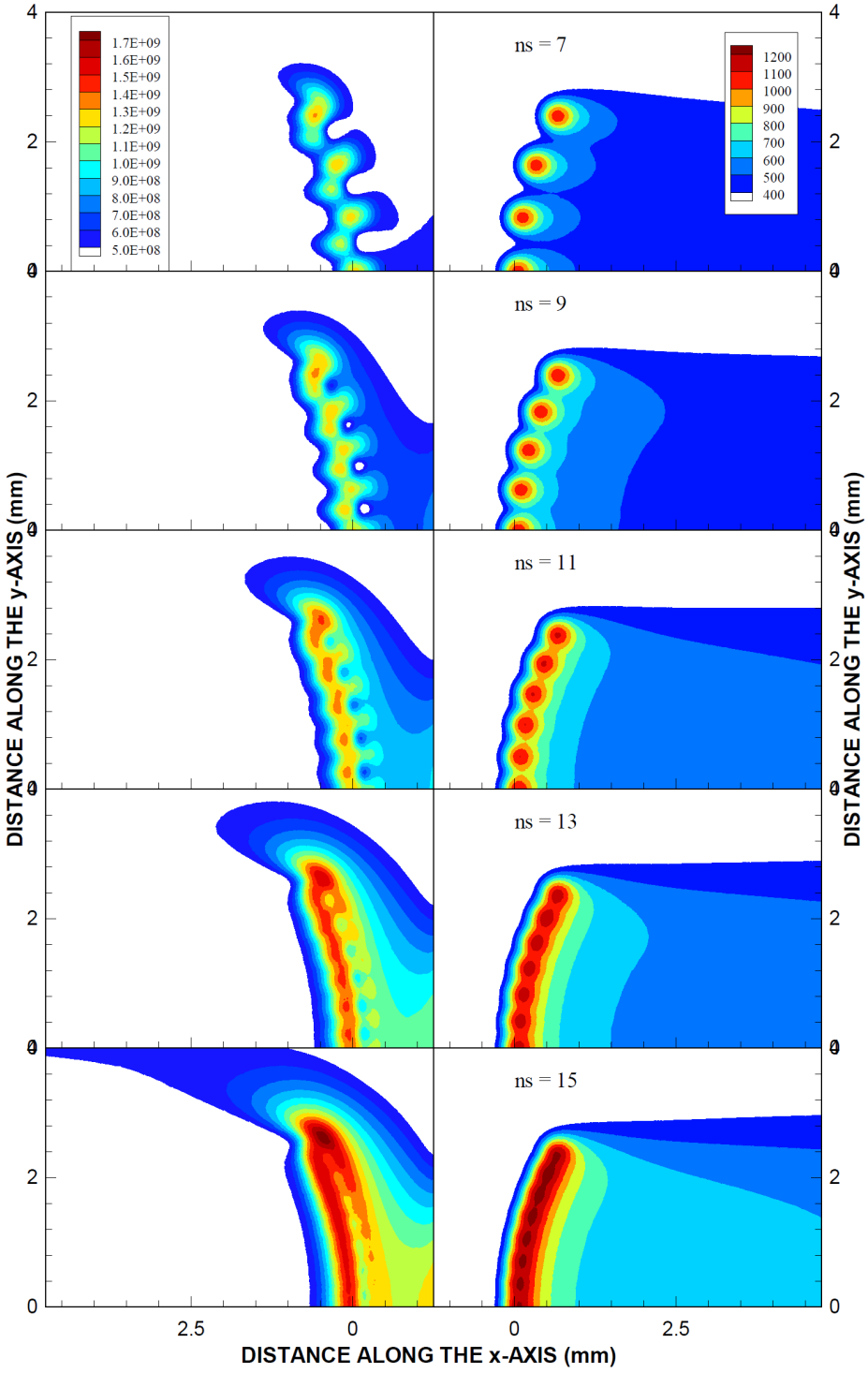

Fig. 2. Temperature and stress contours for various number of laser spots. *ns* represents the number of laser spots.

as the number of irradiated spots increases along the arc length. The difference between the maximum and the minimum von Mises stress becomes small. This, in turn, results in stress continuity along the arc length. Therefore, increasing number of irradiated spots minimizes the local heating and thermal stress field along

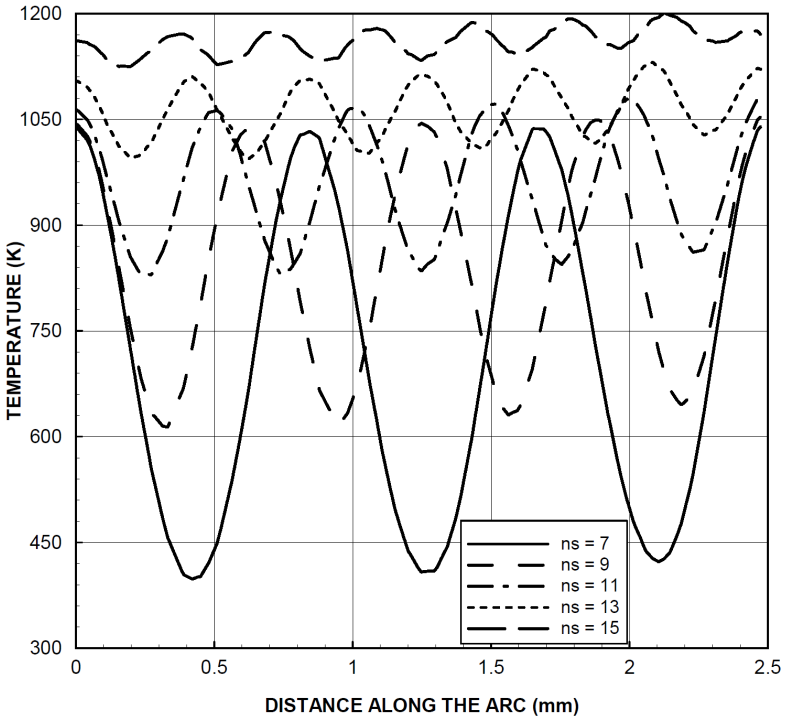

Fig. 3. Temperature distribution along the arc due to various number of spots. *ns* represents the number of spots.

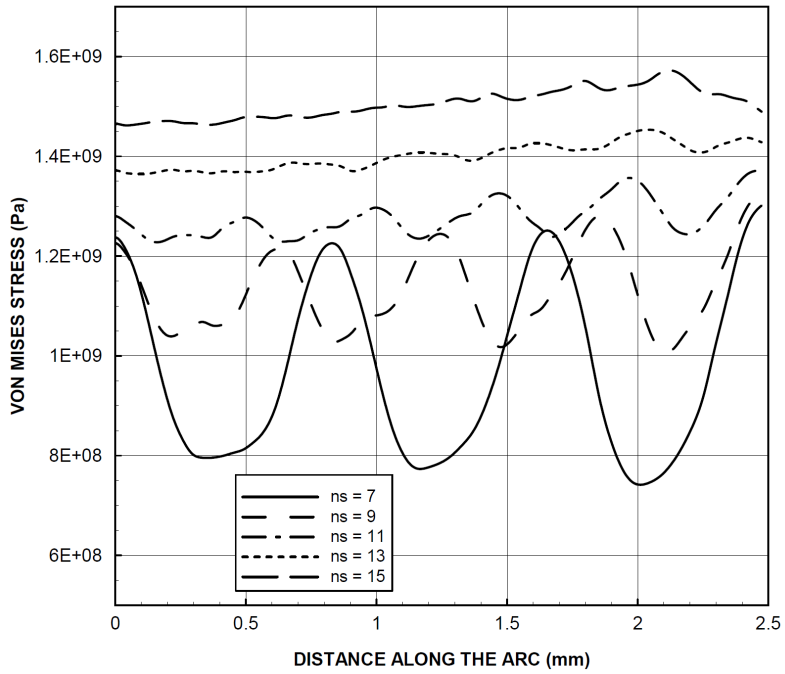

Fig. 4. von Mises distribution along the arc due to various number of spots. *ns* represents the number of spots.

the arc. When comparing difference in von Mises stress due to laser spots 13 and 15, it is evident that both number of spots result in almost the same stress field continuity along the arc, provided that 13 irradiated spots gives rise to less von Mises stress level than that of 15 irradiated spots. Although stress level is high, it is less than the yielding limit of the substrate material.

4. CONCLUSION

Laser multi-beam heating of steel sheet is considered. Effect of number of irradiated spots along the arc length on temperature and stress fields is examined. The arc containing the irradiated spots is assumed to be moving with a constant speed at the workpiece surface along the x-axis. It is found that the number of irradiated spots has significant effect on temperature and stress fields. In this case, local heating is resulted along the arc for less number of irradiated spots. This, in turn, causes high temperature difference between the maximum and the minimum temperatures along the arc length while resulting in local high stress regions along the arc, i.e the difference between the maximum and the minimum von Mises stress is on the order of 400 MPa. As the number of irradiated spots along the arc length increases, difference between the maximum and the minimum temperatures becomes small and high temperature region along the arc length extends almost uniformly. This gives rises to almost uniform high stress region along the arc, i.e., the difference between the maximum and the minimum von Mises stress becomes considerably small. Consequently, introducing multi-spots along the arc length increases heated region at the workpiece surface. The continuity in high temperature and high stress fields along the arc is possible through proper selection of the number of irradiated spots along the arc length.

ACKNOWLEDGEMENTS

Portions of this research were conducted with high performance computing resources provided by King Fahd University of Petroleum & Minerals, Dhahran 31261, Saudi Arabia.

REFERENCES

1. Araghi, B.T., Göttmann, A., Bergweiler, G., Saeed-Akbari, A., Bültmann, J., Zettler, J., Bambach, M. and Hirt, G., "Investigation on incremental sheet forming combined with laser heating and stretch forming for the production of lightweight structures", *Key Engineering Materials*, Vol. 473, pp. 919–928, 2011.
2. Dan, W.J. and Zhang, W.G., "Simulation investigation the effect of heating-lines on tensile mechanical properties of sheet metal after laser scanning", *Advanced Materials Research*, Vols. 314–316, pp. 331–336, 2011.
3. Boley, C.D., Cutter, K.P., Fochs, S.N., Pax, P.H., Rotter, M.D., Rubenchik, A.M. and Yamamoto, R.M., "Interaction of a high-power laser beam with metal sheets", *Journal of Applied Physics*, Vol. 107, No. 4, Article number 043106 (5 pages), 2010.
4. Yanjin, G., Sheng, S., Guoqun, Z. and Yigu, L., "Finite element modeling of laser bending of pre-loaded sheet metals", *Journal of Materials Processing Technology*, Vol. 142, No. 2, pp. 400–407, 2003.
5. Schimek, M., Herzog, D., Kracht, D. and Haferkamp, H., "Laser bead-on-plate welding and overlap seams for increasing the strength and rigidity of high strength steel", *Advanced Materials Research*, Vol. 137, pp. 161–190, 2010.
6. Ueda, T., Wakimura, Y., Furumoto, F., Hosokawa, A. and Tanaka, R., "Experimental investigation on laser flattening of sheet metal", *Optics and Lasers in Engineering*, Vol. 49, No. 1, pp. 137–144, 2011.
7. Chen, M., Lin, K. and Ho., Y., "Laser annealing process of ITO thin films using beam shaping technology", *Optics and Lasers in Engineering*, Vol. 50, No. 3, pp. 491–495, 2012.
8. Kim, J. and Peng., Y., "Plunging method for Nd:YAG laser cladding with wire feeding", *Optics and Lasers in Engineering*, Vol. 33, No. 4, pp. 299–309, 2000.
9. Shuja, S.Z. and Yilbas, B.S., "Pulsative heating of surfaces", *International Journal of Heat and Mass Transfer*, Vol. 41, No. 23, pp. 3899–3918, 1998.